Initial Progress in Developing a Predictive Simulation Tool to Inform Helicopter Ship Operations

Wajih A Memon, Mark D White and Ieuan Owen
University of Liverpool
Liverpool, UK

ABSTRACT

The study presented in this paper is part of the project underway at the University of Liverpool (UoL) to develop a high-fidelity simulation tool that has a predictive capability to inform and support Ship Helicopter Operating Limit (SHOL) trials. The paper reports preliminary progress in developing a desktop based predictive simulation tool that uses a pilot modelling technique to represent the integrated Helicopter Ship Dynamic Interface (HSDI) simulation environment. The approach consists of: a pursuit pilot model, linearized vehicle dynamics, full standard deck landing task, ship motion and equivalent ship airwake turbulence. The tool was initially tested by performing a simplified land-based task for validation purposes. It was then used in HSDI simulations of an SH-60B helicopter operating to a generic single-spot naval frigate. Time and frequency domain comparisons have been made between the predictive tool and piloted simulation flight trials conducted in UoL's Heliflight-R full-motion simulator. It was found that the performance of the predictive tool in maintaining sufficient clearance between the aircraft and the ship whilst rejecting airwake disturbances is well within the desired task performance boundaries. These preliminary investigations show that the tool is capable of representing the dynamics of a pilot in the HSDI environment.

1. INTRODUCTION

The United Kingdom's Royal Navy and Royal Fleet Auxiliary routinely perform helicopter launch and recovery operations to and from their ships. These operations are carried out under challenging at-sea conditions which are unique to the maritime environment. The combination of a confined ship deck landing space, irregular ship motion, sea spray and unsteady airflow over and around the ship's landing deck and superstructure, produce a high risk to, and operational demand on the helicopter, ship and crew. Together, these elements form the HSDI environment [1] (Figure 1).

Figure 1: Helicopter Ship Dynamic Interface Environment

To determine the limitations of the safe operability of helicopters to/from ships, a safety envelope known as the Ship Helicopter Operating Limit (SHOL) is constructed through First of Class Flight Trials (FOCFTs) for every in-service combination of helicopter and ship. The SHOL details the safe conditions for launch and recovery operations, and subsequently provide an operational guideline to the pilot and crew [2]. The larger the SHOL envelope, the greater the operational capability of a given helicopter landing on a given ship. FOCFTs are performed at sea and are inevitably expensive and can typically take weeks to construct a full SHOL envelope. Often the full range of wind and sea conditions (e.g. wind magnitudes and azimuths, sea states) may not be available during at-sea trials, resulting in the development of a conservative SHOL [3]. An example of a SHOL envelope is shown in Figure 2.

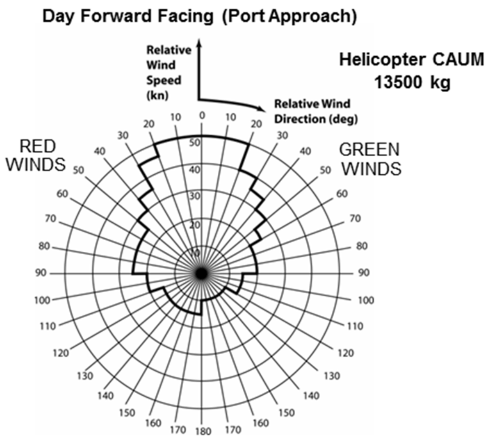

Max Pitch	Max Roll
±2°	±6°

Figure 2: Typical SHOL Diagram

Copyright Statement
The authors confirm that they, and/or their company or organization, hold copyright on all of the original material included in this paper. The authors also confirm that they have obtained permission, from the copyright holder of any third party material included in this paper, to publish it as part of their paper. The authors confirm that they give permission, or have obtained permission from the copyright holder of this paper, for the publication and distribution of this paper as part of the ERF proceedings or as individual offprints from the proceedings and for inclusion in a freely accessible web-based repository.

Presented at 44th European Rotorcraft Forum, Delft, The Netherlands, 19-20 September, 2018

This work is licensed under the Creative Commons Attribution International License (CC BY). Copyright © 2018 by author(s).

The SHOL consists of radial and circumferential lines of wind azimuth and magnitude, respectively, representing the Wind Over Deck (WOD) condition at the deck landing spot. The SHOL limit is shown as a bold black line, and the area inside this boundary indicates the combinations of wind speed/direction for which it is safe to land.

For the reasons detailed above, Modelling and Simulation (M&S) of the HSDI environment is being developed in flight simulators to investigate these operational and meteorological risks, making SHOL testing safer, quicker, and more cost-effective [4-6]. Whilst it is not trying to fully replace at-sea testing, M&S aims to inform the key test points or "Hot Spots" to test at sea.

Over the past few years, flight simulators have been increasingly utilised in deriving helicopter/ship operational guidelines and construction of preliminary simulated SHOL envelopes [7-12], to better understand the complex interaction between helicopter, ship and atmosphere within the HSDI environment. The aim has been to offer a wide range of benefits to the at-sea SHOL development process by testing various HSDI scenarios and environmental conditions repeatedly with a range of pilots, prior to the FOCFTs.

University of Liverpool's Flight Science and Technology research group operates a fully reconfigurable research simulator, Heliflight-R (Figure 3), for the purpose of analysing the flight handling qualities, pilot workload assessment, flight model development and simulation fidelity for land-based and HSDI operations [13]. It has been at the forefront of the research to develop high-fidelity HSDI simulation environments [3, 12]. Heliflight-R has been successfully used in several previous HSDI simulation research projects, such as shipboard operations for simulated SHOL prediction work on a Type-23 Frigate and a Wave Class Auxiliary Oiler [3], HSDI simulation environment development for the Queen Elizabeth Class (QEC) aircraft carrier [11] and Simple Frigate Shape (SFS) helicopter-ship simulations [8].

However, flight simulators, despite their utility, still possess limitations such as the fidelity of motion cue, flight models and hardware complexity all of which may result in compromised task performance and subjective ratings. Moreover, if SHOLs are to be predicted through piloted simulation, a large number of test points are required to effectively capture all the helicopter-ship interactions in different WOD conditions, which is time consuming.

Figure 3: Heliflight-R Simulator (foreground)

In this study, a pilot modelling approach was used to develop an offline desktop predictive simulation tool that will help assess the overall HSDI environment to determine an initial SHOL. The research presented here aims to develop a high-fidelity simulation tool which will have the predictive capability to represent the dynamics of the pilot and flight when operating in the particularly demanding HSDI environment. Moreover, the tool will help to predict and examine mission effectiveness, pilot cueing, environmental effects, and task performance for existing as well as new helicopter-ship combinations. It is intended to use this tool in conjunction with the piloted simulation flight trials performed in the Heliflight-R rotorcraft simulator facility [13] to construct a high-fidelity HSDI simulation framework which will offer a faster, cheaper and more efficient method for operational analysis of shipboard tasks for different combinations of helicopters and ships. The tool is not offered as a substitute to the piloted trials rather it will complement such operations.

Figure 4 shows the predictive tool structure considered in this study which includes a pilot model

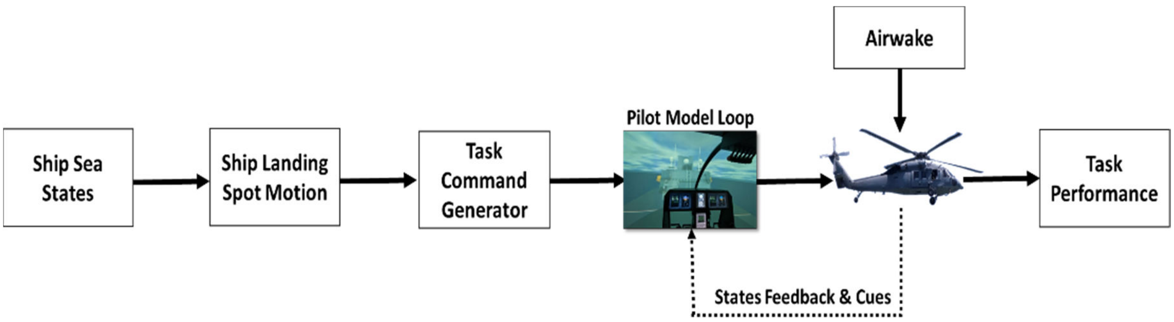

Figure 4: HSDI Predictive Tool Structure

This work is licensed under the Creative Commons Attribution International License (CC BY). Copyright © 2018 by author(s).

loop, helicopter dynamics, human sensory cues feedback, ship airwake and ship motion that represent the integrated HSDI simulation environment.

For the purpose of this paper, two multi-loop flight tasks are examined using the developed tool. The ADS-33E-PRF Precision Hover (PH) task [14] in a near-hover flight condition for the initial analysis, and a full-axis HSDI deck landing task [2] in a low-speed forward flight condition where the mission of interest is the recovery of an SH-60B helicopter to the deck of a generic naval frigate in presence of a ship's airwake and deck motion. The paper is organized as follows: Section 2 discusses existing helicopter-ship desktop simulation tools approaches and their limitations, whilst Section 3 defines the helicopter flight dynamics models used for the two flight conditions considered. Section 4 explains the design procedure of the pilot model loop and Section 5 shows the PH flight task and simulation results. The HSDI task and simulations are shown in Section 6, and finally, conclusion and future work are detailed in Section 7.

2. BACKGROUND OF HSDI M&S PREDICTIVE TOOLS

Various desktop helicopter-ship simulation tools have previously been developed based on a range of pilot modelling techniques. Lee, et al. developed a simulation of a UH-60A GENHEL simulated helicopter operating from a Landing Helicopter Assault (LHA) class ship using a compensatory optimal control pilot model [15]. Moon, et al. investigated the operation of a BO-105 simulated helicopter operating from a TMV 114 fast ferry using a compensatory optimal control pilot model [16], whilst Jarrett, et al. studied the effect of a ship's airwake on an MRH-90 helicopter model recovering to an LHD class ship using a PID controller based virtual pilot model [17].

However, these techniques only partially represent the overall human central nervous system, due to the absence of the additional human sensory modelling elements, particularly the visual, vestibular and proprioceptive systems which provide additional human characteristics to the model. The inclusion of these elements increases the fidelity of the model by approximating the dynamics of the human sensory systems which are important for tasks where the pilot uses information/cues from different perceptual modalities [18] to successfully accomplish the task.

Hess [19] introduced a simplified technique of using a compensatory structural pilot model for modelling helicopter operations near ships which covers all the human sensory feedback systems: vestibular, proprioceptive, visual and neuromuscular dynamics. However, whilst the pilot model is capable of representing a compensatory control strategy, in reality, the helicopter shipboard task is a pursuit tracking task where the target (i.e. the ship's landing deck) is continuously and independently moving [1], imposing additional requirements to the piloted task.

In a compensatory tracking task, a feedback consisting of an indicator and a fixed reference point (i.e. the target) is provided to the pilot and the task is to maintain the indicator on the reference point by compensating for the movements of the indicator via the stick control inputs. An ideal compensatory tracking task would be the one in which there will be no further movement once the target location is achieved. A pursuit tracking task, on the other hand, is one in which the target moves due to external outside influences and the operator controls the follower in such a way as to keep it superimposed over the target. An ideal pursuit tracking would result in continuous movement (e.g. Superslide task [20] and HSDI task [2]). In a pursuit task, the external visual reference and sensory feedback systems are naturally utilized references by the pilot [21, 22].

3. HELICOPTER FLIGHT DYNAMICS

The UoL's Flight Science and Technology research group uses a FLIGHTLAB simulation aircraft model representative of an SH-60B Seahawk helicopter (Figure 5) [23]. The model has been used in several instances for simulated HSDI piloted trials in Heliflight-R simulator, as described in Section 1.

Figure 5: SH-60 Helicopter

Among the different elements of the predictive tool structure shown in Figure 4, one of the critical ingredients required for the successful design of the pilot model loop is a representative linearized flight dynamics model which should accurately capture the dynamics of the vehicle; this was the first step in the design of the predictive tool.

A multi-axis 6 DoF 9-state state-space linearized model (Eqn. 1) of an SH-60 simulated helicopter was extracted from a non-linear FLIGHTLAB model.

$$(1) \qquad \boldsymbol{f}(\boldsymbol{x}, \boldsymbol{x}', \boldsymbol{u}) = 0, \quad \boldsymbol{x} \in \mathrm{R}^9,\ \boldsymbol{u} \in \mathrm{R}^4$$

Presented at 44th European Rotorcraft Forum, Delft, The Netherlands, 19-20 September, 2018

This work is licensed under the Creative Commons Attribution International License (CC BY). Copyright © 2018 by author(s).

Two flight conditions/scenarios were examined within the context of this paper. The first was hover flight trim condition, chosen for initial pilot model gains selection test and preliminary task analysis by simulating the ADS-33E-PRF PH task [14]. The second was the low-speed forward flight condition to simulate the HSDI shipboard landing task [2]. The resulting linear time-invariant system is described by Eqn. 2:

$$x' = \boldsymbol{A}.\boldsymbol{x} + \boldsymbol{B}.\boldsymbol{u} \qquad \boldsymbol{y} = \boldsymbol{C}.\boldsymbol{x} \tag{2}$$

$$\boldsymbol{x} = [\phi, \theta, \psi, u, v, w, p, q, r]$$

$$\boldsymbol{u} = [\delta_{Lat,} \delta_{Long}, \delta_{Coll}, \delta_{Ped}]$$

where x, y and u are the state, output and input vectors, respectively, and *A*, *B* and *C* are the system, input and output matrices, respectively. (ϕ, θ, ψ) are attitudes, (u, v, w) are linear velocities, (p, q, r) are angular rates of the aircraft model and $(\delta_{Lat,} \delta_{Long}, \delta_{Coll}, \delta_{Ped})$ are stick control deflections.

It is important to investigate whether the linearized model is able to represent the behaviour of the full-scale non-linear model. Figure 6, shows the comparison of the linearized SH-60B vehicle model and non-linear full-scale model response to a longitudinal and lateral 3-2-1-1 control input at hover and low-speed flight conditions. Overall, the observed responses of the linearized models show good agreement with the non-linear model.

The linearized model captures the overall behaviour of the helicopter dynamics, which is sufficient for the pilot loop design. The ignored dynamics in the linearized model, such as lead-lag dampers, flapping and inflow possibly account for the slight discrepancies in the off-axis responses. In practice, the sampling time required for the determination of the pilot loop gains to design the pilot feedback loop is shorter than the response time length shown here (approximately up to 4secs), as will be seen in the pilot model loop design in Section 4, Figure 10. Therefore, the agreement between the nonlinear and linearized models for such a short time interval is considered adequate for this application.

4. PILOT MODEL LOOP DESIGN

To improve on the fidelity of existing HSDI desktop tools, such as those described in Section 2, the pilot modelling technique adopted herein to design the SHOL predictive tool was first introduced by Hess and Marchesi [24]. The model is a pursuit pilot tracking model capable of representing multi-loop tasks (two or more control inputs simultaneously) and incorporates all the human sensory equalisation features (e.g. visual, vestibular and proprioceptive system feedback) in a vehicular control manner [26]. These features make the model more applicable to the HSDI launch and recovery operations as it is a complex pursuit tracking task where the pilot derives information/feedback from various sources such as the visual scene, relative aircraft motion and instruments, together with external influencing factors such as airwake disturbances and ship motion [1].

Figure 7 shows the pilot loop structure which includes the vestibular, visual and proprioceptive motion feedback, described previously as sensory equalisation features [24]. The combination of the vestibular-proprioceptive system provides feedback/cues of the attitude rate; the combination of

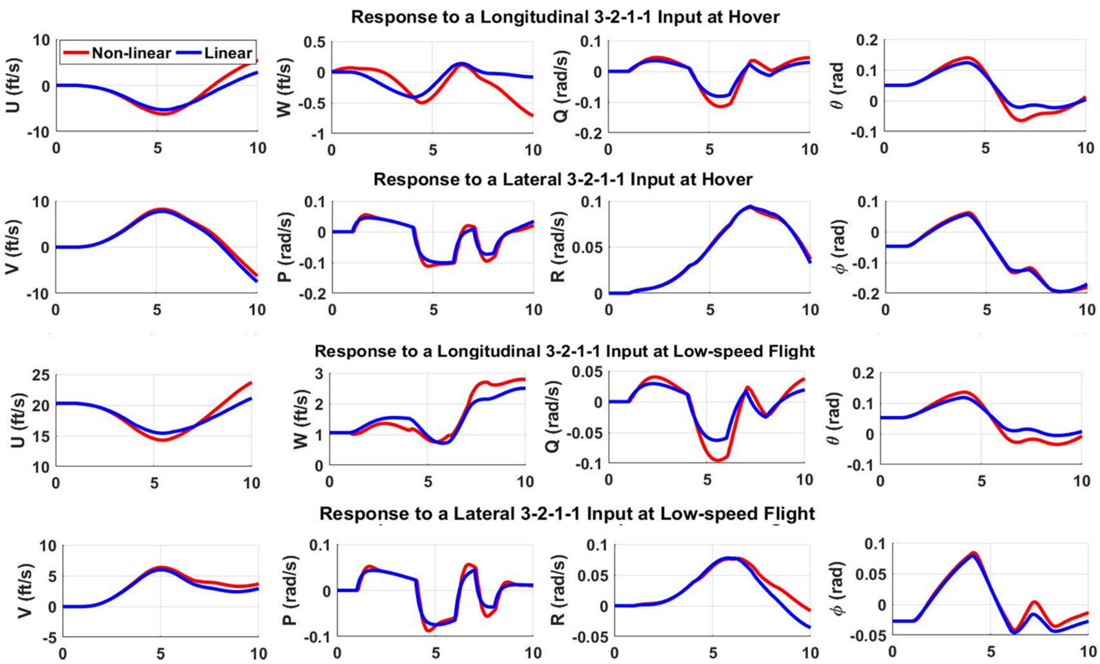

Figure 6: Non-linear and Linear Vehicle Model Comparisons for Hover and Low-speed Flight Conditions

This work is licensed under the Creative Commons Attribution International License (CC BY). Copyright © 2018 by author(s).

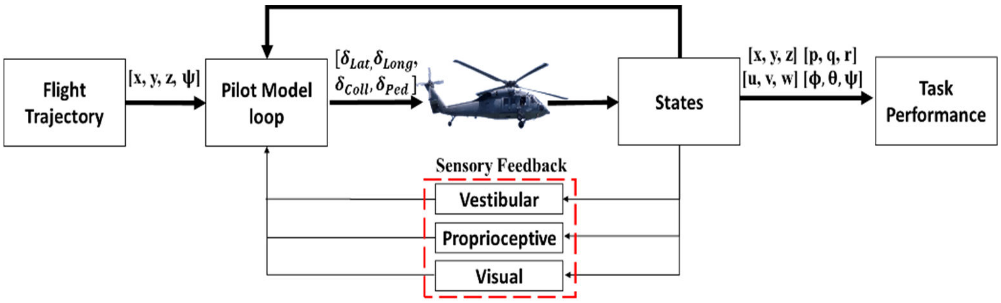

Figure 7: Pilot Model Structure for Motion Sensory Condition

the visual-vestibular system provides attitude cues/feedback. Overall, the sensory feedback provides a good representation of self-motion perception [25, 26].

The pilot model consists of three systems; Command Generator, Pilot Loop and Vehicle Dynamics, as shown in Figure 4. The command generator provides a flight trajectory that is to be followed by the pilot model, consisting of an array of four inputs, x, y, z, ψ (one for each channel). The pilot loop consists of the feedback loops that require the determination of pilot gains using frequency domain (F-D) and/or time domain (T-D) techniques. Vehicle dynamics consist of a linearized state-space model of an SH-60B Helicopter extracted from FLIGHTLAB for a particular flight condition, as described in Section 3. Figure 8 shows the loops of the pilot model. Within each loop, the gain is to be selected based on the requirement that the model should be capable of performing the specified task and should produce representative responses, as close as possible to the real pilot-in-the-loop task. To meet these rules, the gains are selected based on F-D and T-D criteria detailed in the next section.

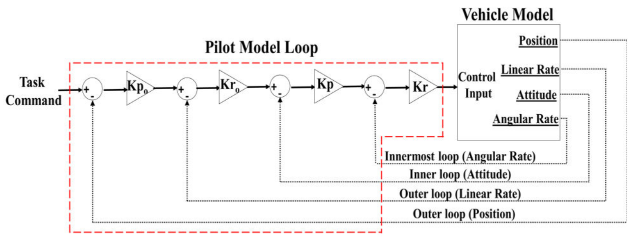

Figure 8: Sequential Pilot Model Loops

4.1. Gain Selection Techniques

To design the pilot model loop, F-D and T-D techniques illustrated in [24] and [27], respectively, were employed for the successful selection of the appropriate pilot gains. The process involves sequentially closing the loops of the pilot model by fulfilling the design requirements within each channel (longitudinal, lateral, collective and pedal) separately, and then combining all the channels to form a 6 DoF pilot model. Altogether there are fourteen pilot gains to be designed, four in each of the lateral and longitudinal channels and three in each of the collective and pedal channels; see Table 1. Figure 8 shows the general multi-loop multi-axis feedback pilot loop structure used in this study to develop the pilot model.

Table 1: Pilot Model Loop Sequence

Channel	Loop Closure Sequence	Channel	Loop Closure Sequence
Longitudinal	$q \rightarrow \theta \rightarrow u \rightarrow x$	Collective	$\dot{w} \rightarrow w \rightarrow h$
Lateral	$p \rightarrow \phi \rightarrow v \rightarrow y$	Pedal	$\dot{r} \rightarrow r \rightarrow \psi$

The successful selection of the pilot loop gains using the F-D technique is based on the fulfilment of the following frequency response requirements in each pilot loop transfer function. Starting from the innermost loop, the gain 'k_r' is selected such that the difference between the peak magnitude response and mid-frequency magnitude is approximately 10dB [24]. The gains 'k_p' and 'k_{ro}' are selected such that the open-loop crossover frequency of the inner and outer loop transfer functions is 2rad/s, and finally the gain 'k_{po}' in the outermost loop is chosen to obtain the crossover frequency of 0.667rad/s (one-third of crossover frequency in inner loop) [24]. The Bode plots in Figure 9 shows the frequency responses obtained from the lateral channel design process, starting from the inner-most (angular rate) closed-loop pilot gain 'k_p', then the inner (attitude) open-loop pilot gain 'k_Φ', then outer (linear rate) loop having pilot gain 'k_v' and finally outermost (translation) loop having pilot gain 'k_y'. The gains are adjusted/tuned until the desired criteria are achieved. The stability of the system is intact since the innermost loop remains closed throughout. This procedure is repeated for all the channels.

The determination of the pilot loop gains can be performed using a T-D technique as well, consisting of an evaluation of the step and sinusoidal responses of the loop transfer functions to the inputs. Figure 10 shows the T-D technique responses obtained from the lateral channel design. The design process is the same as followed in the F-D technique, using sequential loop closure beginning with the innermost loop. A step input of unit amplitude is applied to the innermost loop and the gain 'k_r' is selected at which the ratio of the first overshoot to first undershoot of the response is approximately 2.25 [27], see Figure

Presented at 44th European Rotorcraft Forum, Delft, The Netherlands, 19-20 September, 2018

This work is licensed under the Creative Commons Attribution International License (CC BY). Copyright © 2018 by author(s).

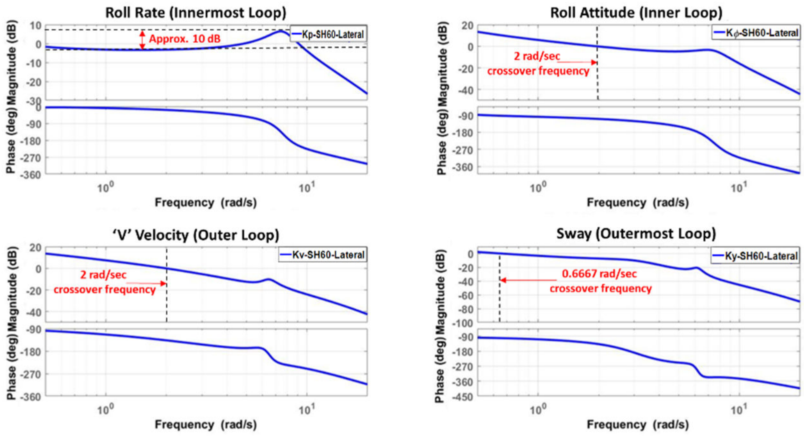

Figure 9: F-D Technique Lateral Channel Pilot Loop Design

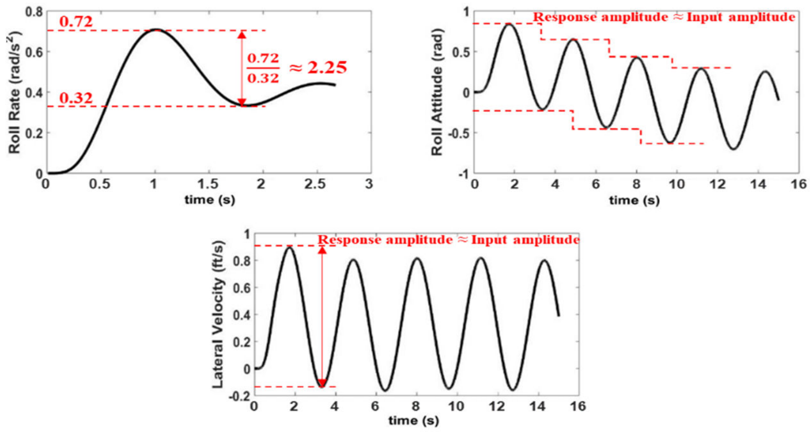

Figure 10: T-D Technique Lateral Channel Pilot Loop Design

10. The gain value obtained can be verified with the Bode plot response obtained using the F-D technique. Once the innermost loop is closed, the inner loop gain 'k_p' is selected by exciting the open loop with a sinusoidal input of a unit amplitude and frequency. The selected gain is the one for which the response amplitude and frequency are approximately the same as the input signal [27], see Figure 10. This is repeated for the outer linear velocity and outermost linear translation loop gains, 'k_{ro}' and 'k_{po}', respectively.

The procedure was followed for determining the pilot gains for both the flight condition, hover and low-speed forward flight.

5. PRECISION HOVER TASK

Following the successful design of the pilot loop, an initial examination was carried out by performing pilot model simulations to compare the responses of the tool with a piloted simulation flight trial for a simple land-based PH task. This was useful to aid in the objective tuning of the pilot gains and analysis of the flight task. The piloted simulation data was acquired from UoL's flight trial database.

The pilot model was devised with a command gener-ator to represent a helicopter pilot performing the PH task. The task course is shown in Figure 11 and an ideal flight trajectory command provided to the tool is shown in Figure 12. The rationale for using this task for the initial model examination was:

a) due to the availability of the sufficient piloted simulation flight trial data and

b) because the PH is a multi-axis closed-loop tracking task in which the lateral and longitudinal axes are both excited and it is useful for translation and position stability performance assessment.

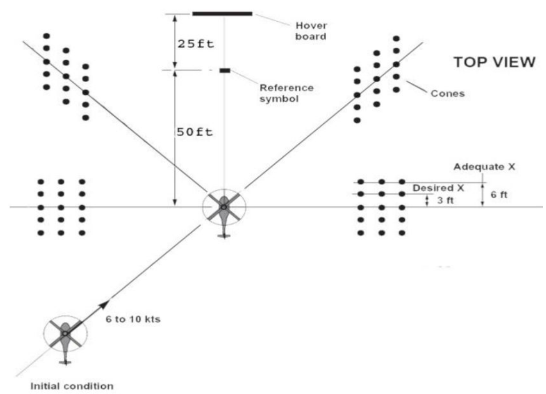

Figure 11: ADS-33E-PRF Precision Hover Task Course [14]

Presented at 44th European Rotorcraft Forum, Delft, The Netherlands, 19-20 September, 2018

This work is licensed under the Creative Commons Attribution International License (CC BY). Copyright © 2018 by author(s).

The commanded task was to initiate the manoeuvre from the stabilized hover condition, at a suitable reference altitude (approximately 20ft), translate longitudinally 90ft and laterally 75ft at a ground speed of between 6 and 10kts and return to stabilized hover, minimising the heading deviations throughout the manoeuvre. The task performance requirements are described in Table 2.

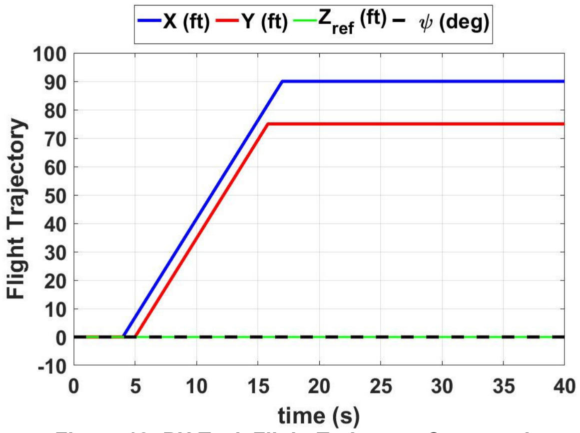

Figure 12: PH Task Flight Trajectory Command

Table 2: ADS-33E-PRF Precision Hover Task Criteria [14]

Criteria	Desired	Adequate
Attain stabilised hover within X secs of initiation of deceleration	5	8
Maintain a stabilised hover for at least X secs	30	30
Maintain the longitudinal and lateral position within ±X feet.	3	6
Maintain heading within ±X°	5	10

5.1. Simulation Results

Figure 13 shows the task performance response of the pilot model tool for the two simulation setups, with ideal trajectory command using originally designed pilot gains (black dashed line) and flight trial trajectory command using optimised pilot gains (red dashed line), compared with the piloted simulation flight trials results. The desired task requirements illustrated in Table 2 were successfully achieved by the tool showing an overall good agreement. However, from the response of the non-optimised condition, it appears that the pilot model loop gains needed a slight tuning in linear velocity loops to further improve the match. Another reason for the slight disagreement is because the pilot model was commanded with an ideal PH task flight trajectory shown in Figure 12. Therefore, for the purpose of testing the ability of the developed tool to reproduce responses similar to that of a real pilot, the pilot model was commanded with the flight trajectory obtained from the piloted simulation flight trial performed in the Heliflight-R simulator and the pilot loop gains were then tuned automatically using MATLAB's "Response Optimisation" toolbox to optimise the match. The gains varied approximately 5-15% from those originally designed. It can be seen that the pilot model reproduces the aircraft responses obtained from the piloted trial very well (red dashed line).

6. HSDI SIMULATION DEVELOPMENT

A preliminary HSDI simulation was developed to perform a full UK standard deck landing task using the developed tool. The operation of the helicopter to a ship was investigated to examine the tool's performance in recovering the helicopter to the moving ship in the presence of the ship's equivalent turbulent airwake and deck motion.

The standard Royal Navy procedure for a port-side forward-facing recovery was adopted as the flight tra-

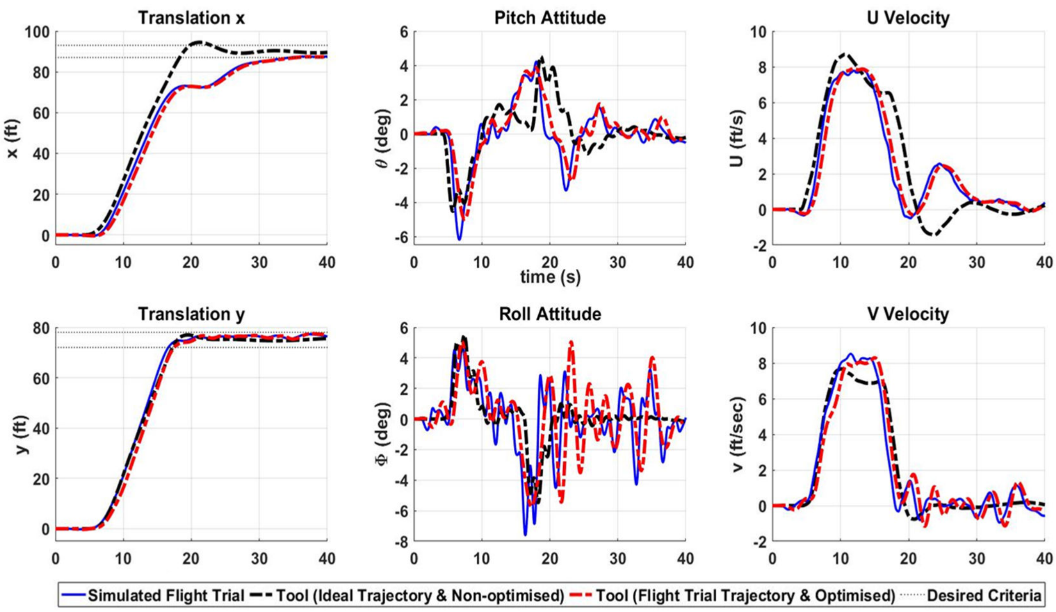

Figure 13: Comparison of Predictive Tool Response and Flight Simulation Trial in PH Task

Presented at 44th European Rotorcraft Forum, Delft, The Netherlands, 19-20 September, 2018
This work is licensed under the Creative Commons Attribution International License (CC BY). Copyright © 2018 by author(s).

-jectory, see Figure 14. This technique requires the pilot to guide the helicopter to a hover position alongside the port side of the ship's deck, followed by a lateral translation to a hover over the deck spot before descending to land on the flight deck [2]. Four (Mission Task Elements) MTEs were identified from this description of the deck landing mission: (i) Approach (ii) Sidestep manoeuvre; (iii) Station-keeping above the flight deck; and (iv) Vertical landing (touchdown).

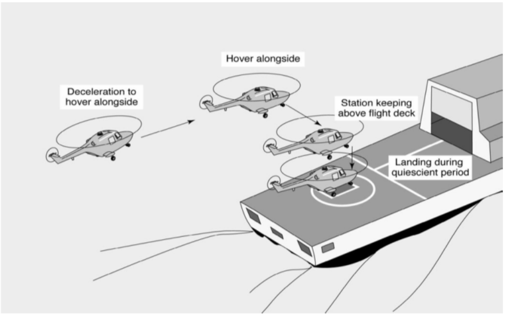

Figure 14: UK RN Standard Deck Landing Approach

The HSDI tool structure consists of the combination of the features shown in Figure 4. The simulation environment approximated, consisted of the low-speed flight linearized vehicle model trimmed at 12kts ground speed with a 13kts headwind to represent 25kts headwind WOD airwake condition, ship motion at 12kts speed Sea State 4 condition and equivalent 25kts WoD airwake representation using the Control Equivalent Turbulence Input (CETI) model [28]. A similar simulation environment had already been developed in the Heliflight-R simulator and the database from piloted simulations carried out by two ex-RN pilots was available for use in the pilot modelling activity [8]. Figure 15 shows the ship's geometry and simulated MTEs.

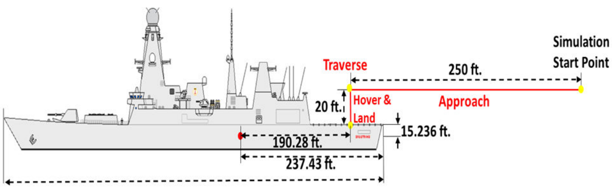

Figure 15: Generic Single-spot Naval Frigate Geometry

The flight trajectory input commanded to the pilot model is shown in Figure 16. The coordinate system is as follows: surge is positive from stern to bow, sway from port to starboard and heave bottom to top. Since the aircraft is trimmed at the same ground speed as the ship (i.e. 12kts) and the simulation start location of the aircraft is 250ft behind the ship landing spot, as can be seen from Figure 15, an initial forward translation command was therefore provided to the aircraft at a constant velocity of 2.77 ft/s for 90 secs to approach alongside the ship's deck and then the ground trim speed of 12kts was maintained, Figure 16.

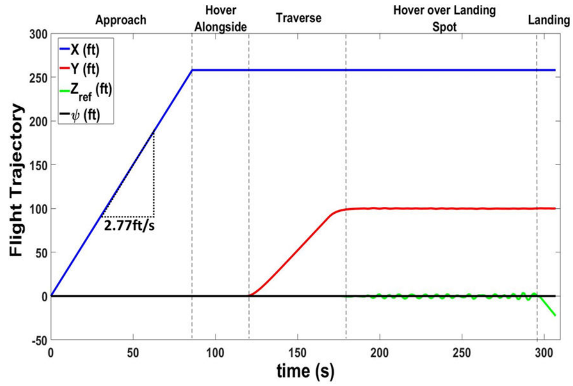

Figure 16: Predictive Tool Input Command for HSDI Task

To account for the ship motion, the landing deck spot's lateral and heave motion shown in Figure 17, serves as a command to the pilot model in the station-keeping MTE portion, as shown in Figure 16. The ship motion was modelled using the ShipMo3D code [8]. It was assumed that the helicopter can land safely on the ship's deck if the pilot model is capable of following its relative position and maintain altitude difference within the safe boundary for a given time. This was examined by the task performance error evaluation, which is detailed in Section 6.1. The ship motion was originally calculated at ship's c.g. and subsequently, the landing spot motion was calculated using Eqns. 3 and 4.

(3) $$Z_{deck} = Z_{c.g} + \sqrt{x_{l2o}^2 + z_{l2o}^2}.\sin\theta_s + z_{l2o}.(1-\cos\phi_s)$$

(4) $$Y_{deck} = Y_{c.g} + x_{l2o}.\sin\psi_s + z_{l2o}.\sin\phi_s$$

$(x_{l2o}, y_{l2o}, z_{l2o})$ are positions from the ship's c.g. location to the landing spot as shown in Figure 15 and $(\phi_s, \theta_s, \psi_s)$ are the ship's roll, pitch and yaw attitude. Figure 17 shows the ship motion calculated at a Sea State 4 condition with a 12kts ship speed.

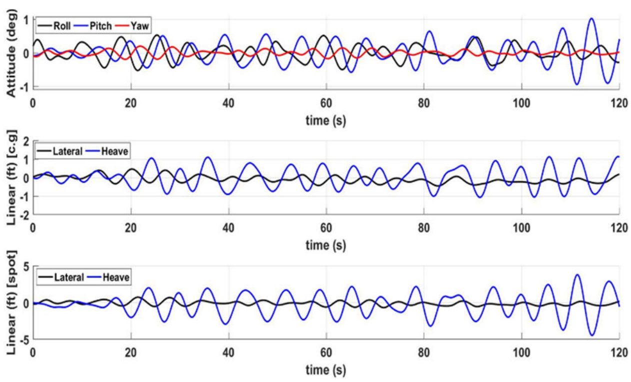

Figure 17: SS4 Ship Motion at c.g. and Landing Spot

The helicopter in the HSDI environment is immersed in the atmospheric turbulence produced by airflow over and around the ship's deck and superstructure. In addition, there is a further wake created due to the rotor of the helicopter that affects the overall airflow generated. Thus, there exists an aerodynamic coupling between helicopter and ship operating in this

Presented at 44th European Rotorcraft Forum, Delft, The Netherlands, 19-20 September, 2018

This work is licensed under the Creative Commons Attribution International License (CC BY). Copyright © 2018 by author(s).

very dynamic environment [8]. However, generating a complete coupled dynamic system takes excessive time and processing power and is not currently possible in real-time piloted simulations. Therefore, in this preliminary study, a CETI model was used. CETI models the general turbulence field by determining the pilot control inputs that can be injected in parallel to the actual control inputs within the model thus producing the aircraft response representative of that produced in the turbulence field. The inputs to the CETI model are the turbulence intensities 'σ', freestream velocity 'U_∞', main rotor radius 'R_m' and tail rotor radius 'R_t'. The CETI model was obtained from the Comprehensive Identification from Frequency Responses (CIFER) tool [28]. The generic CETI model transfer functions are shown in Eqns. 5-8.

(5) $$\frac{\delta_{Lat}}{w_n} = 0.837\sigma_w^{-0.6265}\sqrt{\frac{\sigma_w^2 U_\infty}{\pi R_m}}\left[\frac{1}{s+(2U_\infty/R_m)}\right]$$

(6) $$\frac{\delta_{Long}}{w_n} = 1.702\sigma_w^{-0.6265}\sqrt{\frac{\sigma_w^2 U_\infty}{\pi R_m}}\left[\frac{1}{s+(2U_\infty/R_m)}\right]$$

(7) $$\frac{\delta_{Coll}}{w_n} = 0.1486\sigma_w^{-0.7069}\sqrt{\frac{3\sigma_w^2 U_\infty}{\pi R_m}}\left[\frac{s+33.91(U_\infty/R_m)}{[s+1.46(U_\infty/R_m)][s+9.45(U_\infty/R_m)]}\right]$$

(8) $$\frac{\delta_{Ped}}{w_n} = 1.573\sigma_w^{-0.6265}\sqrt{\frac{\sigma_w^2 U_\infty}{\pi R_t}}\left[\frac{1}{s+(U_\infty/R_t)}\right]$$

Normally, the CETI model produces a constant turbulence intensity field based on a single turbulence intensity RMS value input to the transfer functions illustrated above. However, to represent the spatial variation of turbulence around the ship's flight deck, and therefore improve the fidelity of the airwake disturbance modelling, CFD-computed airwake data for 25kts WoD condition was stored in a 3D lookup table consisting of the full structured airwake domain around the ship. The position of the aircraft relative to the touchdown point on the ship's deck was used to extract airwake velocity data from the look-up tables. Following that, the RMS of the velocity components at every point along the flight path, as shown in Figure 18, were calculated and used as an input into the CETI model hence modifying the original model into an enhanced spatial CETI model.

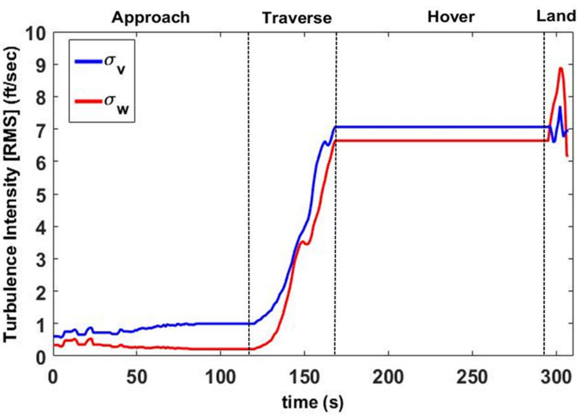

Figure 18: Turbulence Intensities along HSDI flight Path

Figure 19 shows the output of the enhanced CETI model for the turbulence intensities specified in Figure 18. The "baseline" CETI model is not capable of representing the turbulence field in the approach and traverse MTEs of the standard deck landing procedure where the turbulence intensity varies along the flight path, whereas the enhanced model does capture the spatial variation of turbulence intensities in and around the ship.

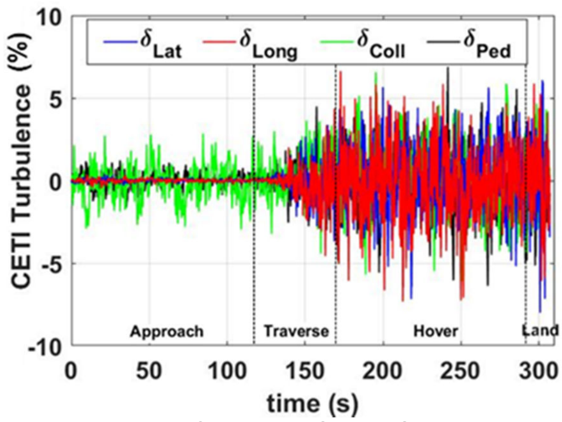

Figure 19: Enhanced CETI Model Output (Spatial Turbulence)

For modelling an airflow field environment, there exists a standard approximate ratio (Eqn. 9) between ambient wind speed, mean wind speed at the landing spot and the turbulence intensity at that point [16, 19]. Eqn. 10 specifies the ratio of the condition simulated.

(9) V : Vr : σ_t = 1:0.4 ~ 0.58:0.05 ~ 0.13 (standard)

(10) V : Vr : σ_t = 1:0.5:0.13 (41.1:20.5:5.5) ft/s

6.1. Simulation Results

Figure 20 shows the simulation results of the developed tool primarily tracking the position of the landing spot, with and without the airwake, for the station-keeping MTE. It can be seen that in both cases, the pilot model tool tracks the ship's heave and lateral motion well and maintains sufficient lateral and vertical clearance from the landing deck. It can further be seen that the airwake (CETI) turbulence has a noticeable disturbance effect on the response of the helicopter, especially in attitude. However, the pilot model successfully accomplishes the task, rejecting the external disturbances whilst maintaining position.

As mentioned earlier, to evaluate the performance of the station-keeping MTE of the overall HSDI task, the task performance can be evaluated by determining the position tracking errors [19]. Figure 21 shows the tracking errors evaluated from one of the simulation runs, which shows that the evaluated position errors (ship deck movement minus aircraft movement) are well within the desired task performance criteria as specified in [19] for a similar dynamic interface task, illustrated in Table 3. The aircraft is expected to remain within an imaginary rectangular box.

Presented at 44th European Rotorcraft Forum, Delft, The Netherlands, 19-20 September, 2018
This work is licensed under the Creative Commons Attribution International License (CC BY). Copyright © 2018 by author(s).

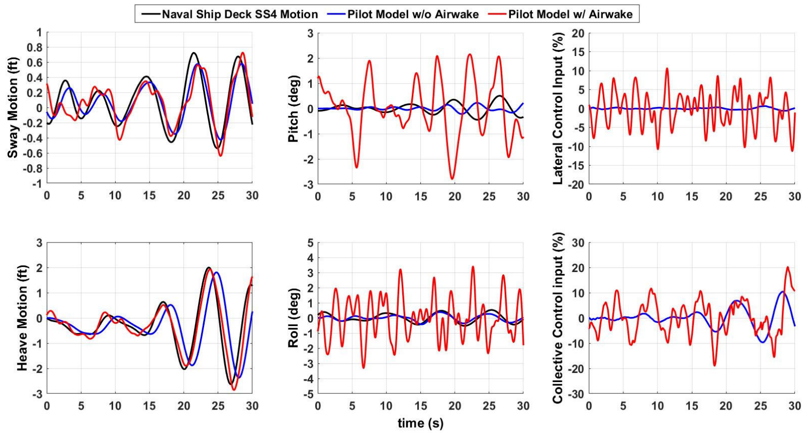

Figure 20: Approximated HSDI Simulation Results using Developed Pilot Model

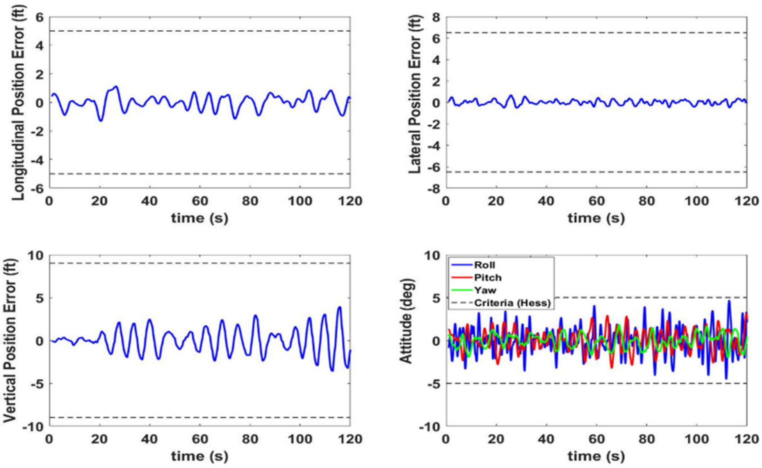

Figure 21: HSDI Pilot Model Task Performance Evaluation through Tracking Errors

Table 3: HSDI Position Tracking Task Performance Criteria [19]

Perf.	X	Y	Z	Attitude
Desired	±5 ft.	±6.5 ft.	±9 ft.	±5°
Adequate	±6.5 ft.	±9 ft.	±12 ft.	±10°

To further analyse the tool's performance, Figure 22 shows the comparison of the FFT of the piloted simulation flight trial and pilot model roll and pitch rate responses during the station-keeping MTE. The overall agreement is representative; however, some discrepancies are apparent which are possibly due to approximations taken within the design of the overall HSDI simulation scenario using the pilot model tool, e.g. linearized vehicle model, equivalent turbulence model and the inclusion of the ship sway and heave motion as a trajectory input to the pilot model within the station-keeping MTE portion. The frequency domain response is expected to improve with the use of more robust modelling techniques which better represent the airwake turbulence computed in CFD and the effect of ship motion. Moreover, the use of a non-linear full-scale flight model will also improve the dynamic response of the vehicle.

Figure 23 shows the comparison of the bode plots identified from the piloted simulation flight trial and predictive tool data for the hover MTE. Two on-axis c--onditions are compared, roll rate response to lateral control input, and pitch rate response to longitudinal control input. It can be seen that the developed tool predicts the responses reasonably well throughout the range of the frequency, 5-50 rad/sec. However, there exist some deficiencies in the pitch rate response which are again possibly due to the model design related approximations discussed in the previous section; these will be further investigated in future work.

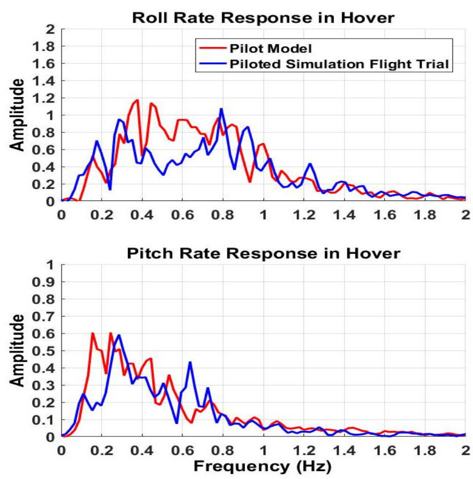

Figure 22: Attitude Rate Response FFT Comparison

Presented at 44th European Rotorcraft Forum, Delft, The Netherlands, 19-20 September, 2018

This work is licensed under the Creative Commons Attribution International License (CC BY). Copyright © 2018 by author(s).

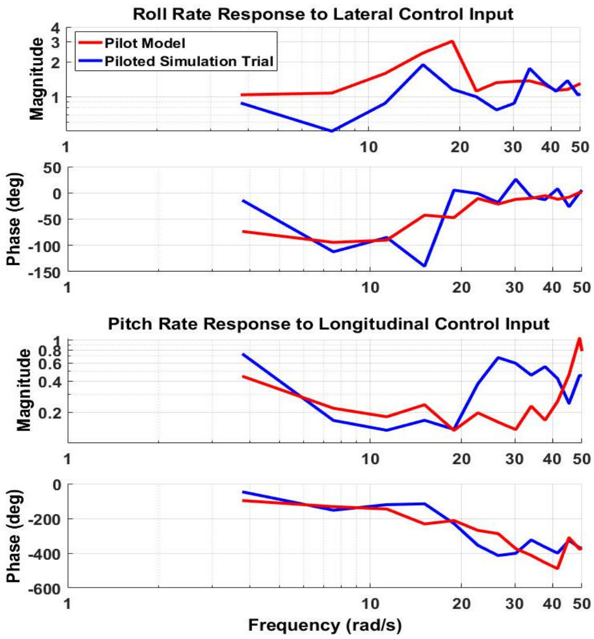

Figure 23: On-axis Identified Bode Plots Comparison

7. CONCLUSIONS AND FUTURE WORK

The research presented in this paper describes preliminary progress towards developing a high-fidelity desktop-based predictive simulation tool that uses a pilot modelling technique to represent the integrated HSDI simulation combining the pilot, vehicle, task and environment elements. A simplified closed-form approach has been utilized, which accounts for the integration of the ship motion and airwake turbulence into the pilot model and can be used for initial shipboard environment modelling and task analysis.

The predictive tool was initially examined for a simple PH land-based task which was shown to be useful for the task analysis and aided in pilot loop tuning. The task performance of the tool compared well with the piloted flight trial simulation. A response optimisation technique was used for the automatic tuning of the pilot loop gains which improved the response match thus demonstrating the tool's ability to reproduce aircraft responses similar to those with a real pilot.

The tool was further evaluated for simulating the HSDI environment with 25kts WoD airwake condition. It was found that in the critical station-keeping MTE, the pilot model was capable of maintaining the desired clearance from the deck while following the lateral and vertical motion of the ship's deck, thus successfully rejecting the external airwake disturbances. Moreover, frequency domain comparisons of the predictive tool and piloted simulation flight trial were examined which showed suitable agreement.

The tool is currently undergoing further development and more robust techniques will be utilised to more efficiently model the HSDI environmental elements and other influencing factors; for example, detailed turbulence modelling techniques will be used for better representation of the airflow around the ship. Also, ship motion interactions will be investigated in detail. In addition, it is intended to perform a three-point comparison between predictive tool, flight simulator and real-world flight trial to improve the fidelity of the tool and to develop further confidence in its use. Finally, it is well understood that the tool is not offered as a substitute for piloted flight trials, it is intended for it to be used in conjunction with simulation and flight trials to quicken the process of deriving shipboard operational guidelines and limitations.

Acknowledgements

The lead author would like to thank the industrial sponsors, QinetiQ and Dstl for funding the project under QinetiQ-Dstl Technology Fund and Sarah Scott a Researcher at the UoL, for access to the ship airwake and piloted simulation flight trial data.

References

[1] Lumsden, B., Wilkinson, C. H. and Padfield, G. D. "Challenges at the Helicopter-Ship Dynamic Interface," 24th European Rotorcraft Forum, Marseilles, France, September 15-17, 1998.

[2] Fang, R., Krijns, H. W. and Finch, R. S. "Dutch/British Clearance Process," RTO AGARDograph 300: Helicopter/Ship Qualification Testing, Vol. 22, Flight Test Techniques Series, NATO Research and Technology Organization, 2003.

[3] Forrest, J. S., Owen, I., Padfield, G. D. and Hodge, S. J. "Ship-Helicopter Operating Limits Prediction Using Piloted Flight Simulation and Time-Accurate Airwakes," *Journal of Aircraft*, Vol. 49, (4), June. 2012, pp. 1020-1031.

[4] Advani, S. and Wilkinson, C. "Dynamic Interface Modelling and Simulation - A Unique Challenge," Royal Aeronautical Society Conference on Helicopter Flight Simulation, London, November 2001.

[5] Roscoe, M. F. and Wilkinson, C. H. "DIMSS - JSHIP's M&S Process for Ship helicopter Testing and Training," AIAA Modeling and Simulation Technologies Conference and Exhibit, California, August 5-8, 2002.

This work is licensed under the Creative Commons Attribution International License (CC BY). Copyright © 2018 by author(s).

[6] Val, J. and Healey, V. "Simulating the Helicopter-Ship Interface as an Alternative to Current Methods of Determining the Safe Operating Envelopes," NAVAIR: Air Vehicle Division, 1986.

[7] Fitzjohn, D., Turner, G. P. and Padfield, G. D. "The Use of Modelling and Simulation in Support of First of Class Flying Trials," Proc. European Rotorcraft Forum, Vol. 2, Marseilles, 1998.

[8] Scott, P., Kelly, M. F., White, M. D. and Owen, I. "Using Piloted Simulation to Measure Pilot Workload of Landing a Helicopter on a Small Ship," 43rd European Rotorcraft Forum, Milan, Italy, September 12-15, 2017.

[9] Lee, D., Sezer-Uzol, N., Horn, J. F. and Long, L. H. "Simulation of Helicopter Shipboard Launch and Recovery with Time-Accurate Airwakes," *Journal of Aircraft*, Vol. 42, No. 2, March-April 2005, pp. 448-461.

[10] Padfield, G. D. and Wilkinson, C. H. "Handling Qualities Criteria for Maritime Helicopter Operations," American Helicopter Society 53rd Annual Forum, Virginia Beach, Virginia, April-May 29–1, 1997.

[11] Kelly, M. F., White, M. D., Owen, I. and Hodge, S. J. "Piloted Flight Simulation for Helicopter Operation to the Queen Elizabeth Class Aircraft Carriers," 43rd European Rotorcraft Forum Proceedings, Milan, Italy, September 12-15, 2016.

[12] Owen, I., White, M. D., Padfield, G, D. and Hodge, S. "A Virtual Engineering Approach to the Ship-Helicopter Dynamic Interface; A Decade of Modelling and Simulation Research at the University of Liverpool," *The Aeronautical Journal*, Vol. 49, (1246), December. 2017, pp. 1833-1857.

[13] White, M. D., Perfect, P., Padfield, G. D., Gubbels, A. W. and Berryman, A. C. "Acceptance Testing And Commissioning of a Flight Simulator for Rotorcraft Simulation Fidelity Research," *Institution of Mechanical Engineers, Part G: Journal of Aerospace Engineering*, Vol. 227, (4), June. 2012, pp. 663–686.

[14] Anon., "Aeronautical Design Standard Performance Specification Handling Qualities Requirements for Military Rotorcraft," ADS-33E-PRF, United States Army Aviation and Missile Command, Redstone Arsenal, AL, 2000.

[15] Lee, D., Uzol, N. S., Horn, J. F. and Long, L. N. "Simulation of Helicopter Shipboard Launch and Recovery with Time-Accurate Airwakes," *Journal of Aircraft*, Vol. 42, (2), April, 2005.

[16] Moon, J., Domercant, J. C. and Mavris, D. "A Simplified Approach to Assessment of Mission Success for Helicopter Landing on a Ship," *International Journal of Control, Automation and Systems*, Vol. 13, (3), August. 2014, pp. 680-688.

[17] Jarrett, D. and Manso, S. "Validation of Simulated Ship Air wake Effects on Helicopter Recoveries," American Helicopter Society 73rd Annual Forum and Technology Displays, Fort Worth, Texas, USA, May 9-11, 2017.

[18] Xu, S., Tan, W., Efremov, A. V., Sun, L. and Qu, X. "Review of Control Models for Human Pilot Behaviour," *Annual Reviews in Control*, Vol. 44, October, 2017, pp. 274-291.

[19] Hess, R. H. "A Simplified Technique for Modelling Piloted Rotorcraft Operations Near Ships," AIAA Atmospheric Flight Mechanics Conference and Exhibit, San Francisco, California, August 15-18, 2005.

[20] Carignan, S., Gubbels, A. and Ellis, K. "Assessment of Handling Qualities for the Shipborne Recovery Task - ADS 33 (Maritime)," 56th American Helicopter Society Annual Forum Proceedings, Virginia Beach, VA, May 1-4, 2000.

[21] Heenan, M. L., Scheidt, R. A. and Beardsley, S. A. "Visual and Proprioceptive Contributions to Compensatory and Pursuit Tracking Movements in Humans," 33rd Annual International Conference of the IEEE EMBS Boston, Massachusetts USA, August 30 - September 3, 2011.

[22] John, W. S. and Marianne, C. "Tracking Performance on Combined Compensatory and Pursuit Tasks," WADC TR 52-39, 1952.

[23] Beck, C. P. and Funk, J. D. "Development and Validation of a Seahawk Blade Element Helicopter Model in Support of Rotorcraft Shipboard Operations," RAeS Rotorcraft Group conference on 'Rotorcraft Simulation', London, UK, May 18-19, 1994.

[24] Hess, R. H. and Marchesi, F. "Simplified Approach for Modelling Pilot Pursuit Control Behaviour in Multi-Loop Flight Control

This work is licensed under the Creative Commons Attribution International License (CC BY). Copyright © 2018 by author(s).

Tasks," *Journal of Aerospace Engineering*, Vol. 220, November, 2006.

[25] Hess, R. H. and Marchesi, F. "Analytical Assessment of Flight Simulator Fidelity Using Pilot Models," *Journal of Guidance, Control, and Dynamics,* Vol. 32, No. 3, 2009, pp. 760-770.

[26] Hess, R. H. "Model for Human Use of Motion Cues in Vehicular Control". *Journal of Guidance, Control, and Dynamics,* Vol. 13, No. 3, 1990, pp. 476-482.

[27] Hess, R. A. "Obtaining Multi-Loop Pursuit-Control Pilot Models from Computer Simulation," Proceedings of the Institution of Mechanical Engineers, Part G: *Journal of Aerospace Engineering*, Vol. 222, No. 2, 2008, pp. 189–200.

[28] Lusardi, J., Tischler, M. B., Blanken, C. L. and Labows, J. S. "Empirically Derived Helicopter Response Model and Control System Requirements for Flight in Turbulence," American Helicopter Society 56th Annual Forum, Fort Worth, Virginia Beach, VA, May 1-4, 2000.

Presented at 44th European Rotorcraft Forum, Delft, The Netherlands, 19-20 September, 2018

This work is licensed under the Creative Commons Attribution International License (CC BY). Copyright © 2018 by author(s).